Pifithrin-alpha has a p53-independent cytoprotective effect on docosahexaenoic acid-induced cytotoxicity in human hepatocellular carcinoma HepG2 cells

Syu-ichi Kanno *, Kaori Kurauchi, Ayako Tomizawa, Shin Yomogida, Masaaki Ishikawa

Department of Clinical Pharmacotherapeutics, Tohoku Pharmaceutical University, 4-4-1 Komatsushima, Aobaku, Sendai 981-8558, Japan

HIGHLIGHTS

- Pifithrin-alpha (PFT) blocked docosahexaenoic acid (DHA)-induced cytotoxicity.
- The inhibitory effect of PFT on DHA-induced cytotoxicity was regardless of p53.
- PFT markedly inhibited DHA-induced induction of oxidative activity and autophagy.
- PFT significantly suppressed the mitochondrial damage by DHA.
- Our data suggests that PFT has a p53-independent inhibition mechanism.

ABSTRACT

Pifithrin-alpha (PFT) is an inhibitor of p53 and is known to protect against a variety of p53-mediated genotoxic agents. In this report, we examined the inhibitory effects of PFT against docosahexaenoic acid (DHA)-induced cytotoxicity in the human hepatocellular carcinoma (HCC) cell line HepG2. PFT significantly abrogated DHA-induced cytotoxicity in wild-type HepG2 cells (normal expression of p53) and after p53-knockdown by siRNA, as well as in Hep3B (p53 null) and Huh7 (p53 mutant) cells. DHA-induced cytotoxicity is mediated by induction of oxidative stress, and PFT inhibited this event, but it does not exert antioxidant effects. PFT significantly suppressed the release of cytochrome c from mitochondria to cytosol, as well as changes in the mitochondrial membrane potential ($\Delta\Psi_M$) by DHA. Therefore, protection of mitochondria by PFT is crucial for its inhibition of DHA-induced cytotoxicity. Although it has been reported that PFT is able to block p53 function, our data suggest that PFT also has a p53-independent inhibition mechanism. This work provided insights into the mechanisms of PFT action on DHA-induced cytotoxicity in HCC.

© 2014 The Authors. Published by Elsevier Ireland Ltd. This is an open access article under the CC BY-NC-ND license (http://creativecommons.org/licenses/by-nc-nd/3.0/).

1. Introduction

The tumor suppressor p53 is generally viewed as the most direct and promising anti-cancer target. Although p53 as a transcriptional factor is best known for controlling the cell cycle and apoptosis, increasing evidence suggests that p53 is also involved in induction of autophagy (Guo et al., 2013). The pharmacological rescue of inactive p53 may therefore represent an attractive therapeutic approach. Pifithrin-alpha (PFT) is an inhibitor of p53 and is considered to be useful for therapeutic suppression in order to reduce cancer treatment side effects (Komarova and Gudkov, 1998) and to protect against various genotoxic agents (Komarova et al., 2003). Several reports have shown that PFT blocks the p53-mediated activation of autophagy caused by chemical agents (Dong et al., 2012; Zhu et al., 2011). PFT has been validated as a useful p53 inhibitor for the elucidation of p53 functions in experimental studies.

It has been observed that docosahexaenoic acid (DHA), an omega-3 polyunsaturated fatty acid, causes cancer cell death via apoptosis (Gleissman et al., 2010; Lim et al., 2009; Wendel and Heller, 2009). Along with apoptosis, autophagy has been indicated to play a role in the cytotoxic mechanisms of DHA in recent reports (Jing et al., 2011; Rovito et al., 2013; Yao et al., 2014). Autophagy and apoptosis are self-destructive processes

* Corresponding author. Tel.: +81 22 727 0112; fax: +81 22 275 2013.
E-mail address: syu-kan@tohoku-pharm.ac.jp (S.-i. Kanno).

that share many key regulators, such as reactive oxygen species (ROS). Physiological levels of ROS lead to growth adaption and survival; however, excess ROS cause irreversible cellular damage, thus provoking autophagy and/or apoptosis (Droge, 2002; Rubio et al., 2012). It has been shown that production of ROS is a key mediator of DHA-induced cytotoxicity (Arita et al., 2001; Maziere et al., 1999). A previous report has also shown that DHA-induced cytotoxicity is mediated by oxidative stress, and the cytotoxic effects are abrogated by typical antioxidants (Kanno et al., 2011). Currently, DHA has potential applications in chemotherapy; phase II clinical trials and randomized phase III trials are currently underway (Hajjaji and Bougnoux, 2013). Hepatocellular carcinoma (HCC) is the fifth most common form of cancer worldwide and the third most common cause of cancer-related deaths (Raza and Sood, 2014). Safe and effective chemotherapeutic reagents such as DHA are needed for use against HCC, and it remains important to elucidate the cytotoxic mechanisms of DHA against HCC.

As mentioned above, there have been several studies on the cytotoxic mechanisms of DHA and the p53-dependent inhibitory effects of PFT using experimental cell culture models, but it is unknown whether PFT affects DHA-induced cytotoxicity in human HCC cells. In this report, we examined the effects of PFT on DHA-induced reductions in cell survival in HepG2 cells, as well as the effects on p53 expression, oxidative stress, autophagy and mitochondrial damage. This is the first report to suggest that PFT acts via a p53-independent mechanism against DHA-induced cytotoxicity in HepG2 cells.

2. Materials and methods

2.1. Cell cultures and reagents

Human hepatoma HepG2, Hep3B or Huh7 cells were supplied by the Cell Resource Center for Biomedical Research, Tohoku University (Sendai, Japan). Cells were routinely kept in RPMI 1640 medium supplemented with 10% fetal bovine serum and penicillin G (100 U/ml)/streptomycin (100 μg/ml) at 37 °C in a humidified 5% CO_2-95% air incubator under standard conditions.

The drugs used in these experiments, pifithrin-α (PFT) or cis-4, 7, 10, 13, 16, 19-DHA (#D2534, ≥98%; Sigma, St. Louis, MO) and all other reagents were of the highest grade available, and were supplied by either Sigma or Wako Pure Chemical Industries (Osaka, Japan). Cell culture reagents were obtained from Life Technologies[TM] (Carlsbad, CA). DHA was dissolved in ethanol and stored as a 200 mM stock solution, flushed with argon, in lightproof containers at −20 °C. Light exposure was kept to a minimum for all drugs used. All antibodies using for Western blotting were purchased from Cell Signaling Technology (Danvers, MA).

2.2. p53 siRNA knockdown assay

siRNA-p53 (si-p53) and siRNA-control (non-targeting siRNA; negative control [Neg]) were transfected into HepG2 cells using HyperFect transfection reagent (Qiagen, Valencia, CA) according to the protocol supplied by the manufacturer. A non-targeting siRNA was used as a control for the non-sequence-specific effects of transfected siRNAs. The siRNAs (Qiagen) used were si-p53 from FlexiTube siRNA (catalog no. SI00011655) and negative control from AllStars Neg. Control siRNA (catalog no. SI03650318). Briefly, 5×10^4 HepG2 cells containing each siRNA (final concentration, 10 nM) and HyperFect reagent were incubated for 24 h for assessment of p53 expression or cytotoxic effects by DHA.

2.3. RNA isolation and quantitative real-time polymerase chain reaction assay

In order to confirm knockdown by siRNA in HepG2 cells, expression levels of p53 messenger RNA (mRNA) (GenBank Accession no. NM_000546.5) were quantified by real-time polymerase chain reaction (qPCR) with Light Cycler (Roche, Basel, Switzerland). Briefly, after transfection with siRNAs for 24 h in HepG2 cells, total RNA was extracted from each cell line by ISOGEN reagent (Nippon Gene, Tokyo, Japan), and RNA concentrations were determined by NanoDrop 1000 (Thermo Fisher Scientific, Inc., Waltham, MA). From each sample, 0.1 μg of total RNA was then reverse transcribed into single-strand cDNA using an RverTra Ace® qPCR RT Kit (Toyobo, Osaka, Japan). Aliquots of cDNA preparations were then subjected to qPCR analysis on KOD SYBR® qPCR Mix (Toyobo) in order to quantitate the gene expression of p53 and β-actin (GenBank Accession no. NM_001101.3, internal standard) using Light Cycler. Primer pairs were from the QuatiTect® Primer Assay (p53, #QT00060235 or β-actin, #QT00095431; Qiagen, Valencia, CA). The results of all assays were checked against melting curves in order to confirm the presence of single PCR products. At least two independent experiments were conducted and at least triplicate samples were used in each experiment.

2.4. Western blotting

Cells were washed with phosphate buffered saline (PBS) and lysed in CelLytic M® (Sigma) in order to collect total cell lysates, cytosol was separated and mitochondrial protein fractions were collected using the Mitochondria Isolation Kit® (Sigma) according to the manufacturer's instructions. Protein concentrations were measured using a BCA[TM] protein assay kit (Thermo Fisher Scientific, Inc.) in accordance with the manufacturer's instructions. Samples of each protein (30 μg of whole cell lysates, and 5 μg of either cytosol or mitochondrial protein) were loaded onto a 10–15% SDS-polyacryl-amide gel. After electrophoresis, proteins were transferred to a polyvinylidene difluoride (PVDF) membrane. Protein was blocked with Blocking One® (Nacalai Tesque Inc., Kyoto, Japan) for 1 h, and was reacted with antibody overnight at 4 °C. Membrane was then washed with buffer (PBS containing 0.05% Tween-20), followed by incubation with horseradish peroxidase-linked secondary antibody for 1 h. After washing, protein levels were analyzed by enhanced chemiluminescence with Pierce® Western blotting substrate (Thermo Fisher Scientific, Inc.).
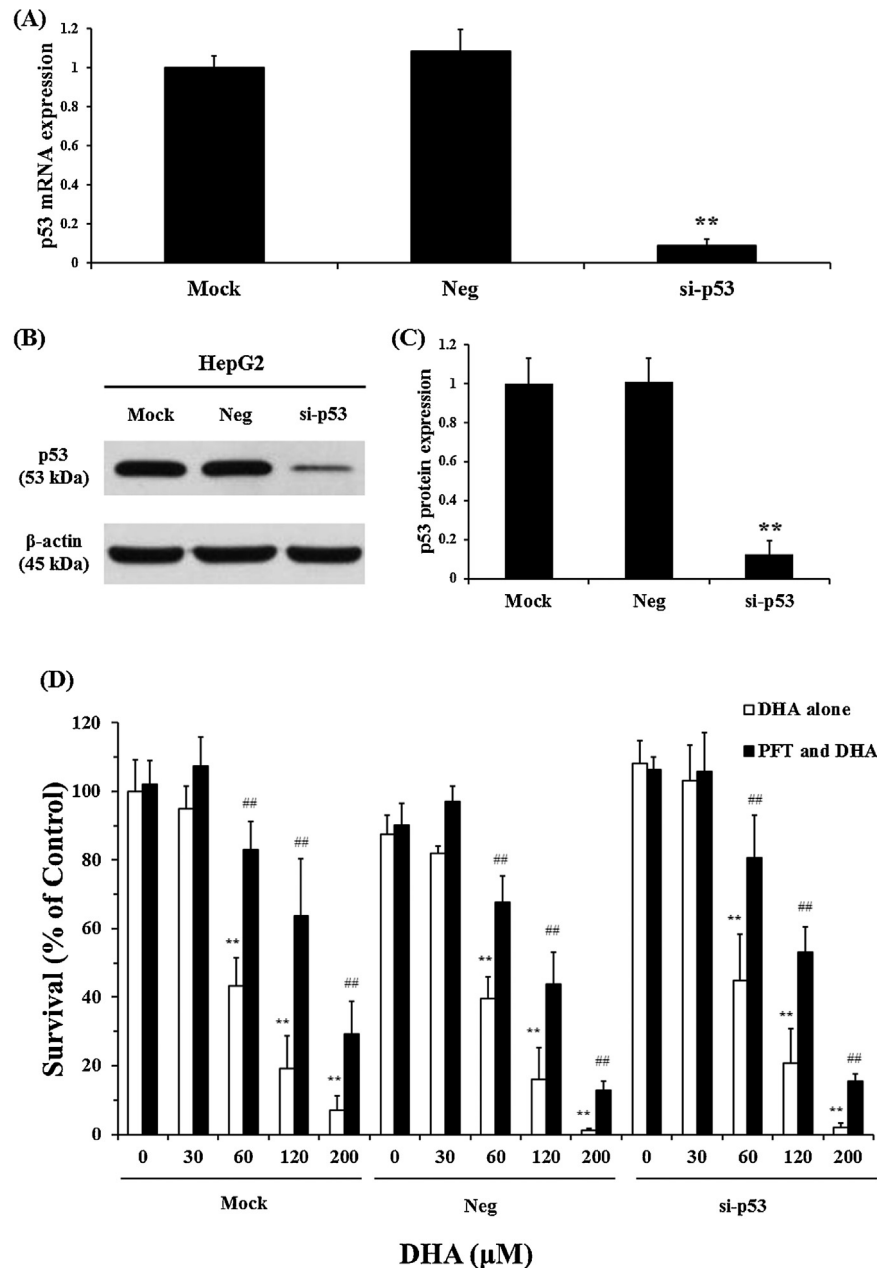
2.5. Cytotoxicity

Cytotoxicity was assessed by the water-soluble tetrazolium (WST-1; sodium 5-(2,4-disulfophenyl)-2-(4-iodophenyl)-3-(4-nitrophenyl)-2H tetrazolium inner salt) assay, which detects metabolically competent cells with an intact mitochondrial electron transport chain (Berridge et al., 2005). Briefly, 1×10^4 cells were seeded into 96-well plates and cultured overnight. Cells were pre-treated with PFT for 1 h, followed by incubation with DHA for the indicated times, and addition of medium containing WST-1 solution (0.5 mM WST-1 and 0.02 mM 1-methoxy-5-methylphenazinium methylsulfate; 1-PMS) to each well. Cells were incubated for 60 min at 37 °C, and absorption at 438 nm (reference 620 nm) was measured using a SH-1200 Microplate Reader® (Corona, Hitachinaka, Japan). Control cells were treated with 0.1% ethanol. Cell viability was calculated using the formula: absorbance in treated sample/absorbance in control $\times 100$ (%).

2.6. Measurement of oxidative stress

Intracellular oxidative stress was evaluated by measuring intracellular peroxide-dependent oxidation of 2′,7′-dichlorodihydrofluorescein diacetate (DCFH-DA) to form the fluorescent compound, 2′,7′-dichlorofluorescein (DCF), as described previously (Kanno et al., 2011). Results are expressed as a percentage of fluorescence intensity with respect to the control.

2.7. Total antioxidant capacity (TAC) assay

An oxidation system comprising 2,2′-azino-di (3-ethylbenzthiazoline-6-sulfonic acid) (ABTS), myoglobin and hydrogen peroxide (H_2O_2) has been used for TAC assay to determine Trolox equivalent antioxidant capacity (Kambayashi et al., 2009; Yu and Ong, 1999). We used this assay to assess the antioxidant capacity of PFT. Briefly, 90 μL of 10 mM phosphate buffered saline (pH 7.2),

Fig. 1. Effects of PFT on DHA-induced cytotoxicity in wild-type p53-expressing or p53 knockdown HepG2 cells. Each sample was transfected with (Neg: negative control; si-p53: p53) or without (Mock) siRNA. (A) Effects of p53 knockdown by siRNA on p53 mRNA expression in HepG2 cells were assessed by quantitative real-time polymerase chain reaction (qPCR). Results of qPCR are expressed as fold change in mRNA levels relative to Mock, using β-actin as an endogenous housekeeping gene. (B) Representative results of Western blotting from three independent experiments. Each sample (n = 3–5) was extracted after transfection with siRNA for 24 h in HepG2 cells. Samples containing 30 μg of protein were loaded onto 10% SDS-PAGE, and blots were probed with corresponding antibodies. β-actin levels were used as a loading control. (C) Data are means ± SEM of relative expression levels of p53 protein from three samples. **$p < 0.01$ compared with Mock group. (D) siRNAs transfected into HepG2 cells were incubated for 24 h, followed by DHA treatment and examination for survival at 24 h. DHA-induced cytotoxicity in HepG2 cells was estimated by WST-1 assay. Survival (%) was calculated relative to no DHA incubation (Mock). Results are expressed as means ± SEM of three samples. White bars (□): single incubation with DHA; black bars (■): pretreatment with PFT at 20 μM for 1 h, and DHA incubation for 24 h at the indicated concentrations. **$p < 0.01$ compared with controls for each siRNA-transfected cell group; ##$p < 0.01$ compared with the indicated concentrations of single incubation with DHA.

50 μL of myoglobin solution, 20 μL of 3 mM ABTS solution, and 20 μL of PFT or Trolox solution were added to 96-well microplates. Reactions were started by addition of H_2O_2 (final concentration: 250 μM), and were followed at 600 nm with a microplate reader for 10 min.

2.8. Immunofluorescence assay as confocal fluorescence microscopy for detection of protein 1 light chain 3 (LC3) and cytochrome c

Cells were seeded into the Lab-Tek® 8-well chambered cover glass system (Thermo Fisher Scientific, Inc.) at densities of 2×10^4, and were incubated overnight under standard culture conditions. Cells were pre-treated with or without PFT at 20 μM for 1 h, followed by incubation with DHA at 120 μM for the indicated times. Chambered slides were washed twice with phosphate buffered saline (PBS). For detection of protein 1 light chain 3 (LC3), cells were fixed in ice-cold 1:1 methanol:acetone for 30 min. Slides were immersed for 50 min in 1% goat serum and 0.1% Triton X-100 in PBS, and were then transferred to 10% goat serum/PBS for 20 min. Following the PBS rinse, slides were incubated with primary antibody (anti-LC3; MBL, Nagoya, Japan) at 1:1000 in PBS for 1 h at room temperature, washed with PBS, and then incubated with fluorescein isothiocynate (FITC)-conjugated anti-rabbit secondary antibody (Beckman Coulter, Brea, CA) for 30 min. For detection of cytochrome c, after incubation with reagents, the medium was removed and cells were fixed in Mildform® (Wako, Osaka, Japan) for 10 min. Slides were immersed for 5 min in 0.1% Triton X-100 in PBS and were then transferred to 3% FBS/PBS for 30 min. After washing with PBS, slides were incubated with Alexa Fluor® 555 mouse anti-cytochrome c antibody (BD Pharmingen™, San Jose, CA) at 1:40 in PBS for 1 h. After incubation with antibodies, rinsing with PBS and a drop of UltraCruz™ Mounting Medium with DAPI (Santa Cruz Biotechnology, Inc., Dallas, TX) was added to each well. Cells were observed under a confocal fluorescence microscope (C-1; Nikon, Tokyo, Japan) for blue fluorescence intensity (405 nm) indicating the nucleus, green fluorescence intensity (488 nm) indicating LC3-positive cells (indicative of autophagy), or red fluorescence intensity (562 nm) indicating expression of cytochrome c.

2.9. Mitochondrial membrane potential ($\Delta\Psi_M$) assay

In order to detect the effects of PFT and DHA on mitochondrial membrane potential ($\Delta\Psi_M$) in HepG2 cells, we used the Cell Meter JC-10 mitochondrial membrane potential assay kit (AAT Bioquest®, Inc., CA). JC-10 is capable of selectively entering the mitochondria, and reversibly changes its color from orange to green based on membrane potential. This property is due to the reversible formation of JC-10 aggregates on membrane polarization that causes shifts in emitted light from 527 nm (i.e., emission of JC-10 monomeric form) to 590 nm (i.e., emission of J-aggregate form). Briefly, cells were seeded at a density of 5×10^3 in Nunc 96 MicroWell™ optical bottom plates (Thermo Fisher Scientific, Inc.) or into the Lab-Tek® 8-well chambered cover glass system (Thermo Fisher Scientific, Inc.) at densities of 2×10^4, and were incubated overnight under standard culture conditions. After treatment with PFT and DHA for the indicated times, cells were incubated with JC-10 dye-loading solution for 30 min, and fluorescence intensity in each well on the 96-well plates was determined using a TECAN infinite® M1000 microplate reader (Tecan Group Ltd.), or the cells were observed under a confocal fluorescence microscope C-1 (Nikon) for green fluorescence intensity (JC-10 monomeric form) or orange fluorescence intensity (J-aggregate form). The aggregate/monomer ratio is assumed to be proportional to $\Delta\Psi_M$ intensity (Reers et al., 1995).

2.10. Statistical analysis

Statistical analysis was performed by one- or two-way analysis of variance (ANOVA), followed by Williams' type multiple comparison test or the Bonferroni test among multiple groups. Data are expressed as means ± standard error of the mean (SEM). A p-value of less than 0.05 was considered to be significant.

3. Results

3.1. PFT decreased DHA-induced cytotoxicity independent of p53 expression in HCC cells

First, in order to confirm the effects of PFT against DHA-induced cytotoxicity in HepG2 cells (wild-type expression of p53), we established p53-knockdown HepG2 cells using siRNA (Fig. 1). After transfection of HepG2 cells with siRNA-p53 (si-p53) for 24 h, expression levels of p53 were significantly lower at both the mRNA (Fig. 1A) and protein (Fig. 1B and C) levels when compared to the treatment control group (treatment with transfection reagent; Mock) and the transfection control group (treatment with non-targeting siRNA; negative control; Neg). Transfection with siRNA did not affect cell survival. We examined the cytotoxic effects by assessing mitochondrial activity (i.e., WST-1 assay). After transfection with or without siRNA for 24 h, and following incubation with DHA for 24 h, reductions in cell survival with DHA at 60, 120 or 200 μM were 43.2 ± 8.3, 19.2 ± 9.6 or $7.1 \pm 4.3\%$, respectively, when compared to the Mock group (Fig. 1D). Single incubation with DHA concentration-dependently reduced cell survival to a similar degree after transfection with Neg and si-p53. These cytotoxic effects showed no significant differences with the Mock group. In the Mock group, PFT significantly decreased DHA-induced cytotoxicity at 60, 120 or 200 μM (83.1 ± 8.2, 63.7 ± 16.5 or $29.3 \pm 9.6\%$, respectively; $p < 0.01$), and this inhibition was observed after transfection with Neg and si-p53. To further evaluate the effects of PFT on DHA-related effects, we examined DHA-induced cytotoxicity in cells with different p53 expression states; Hep3B (p53 null cells) and Huh7 (p53 muted cells).
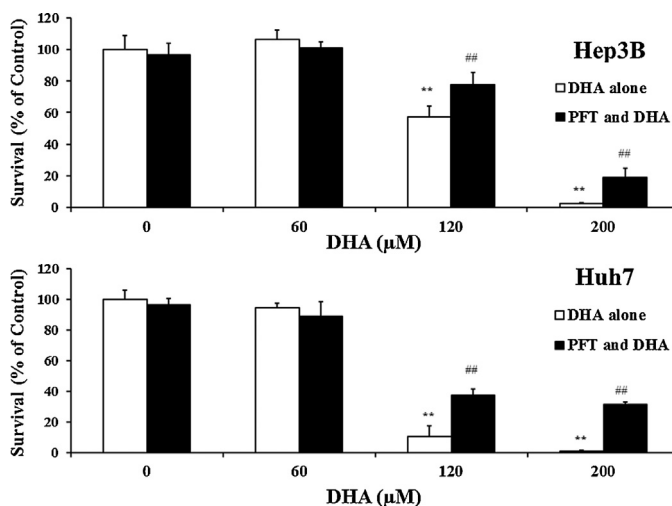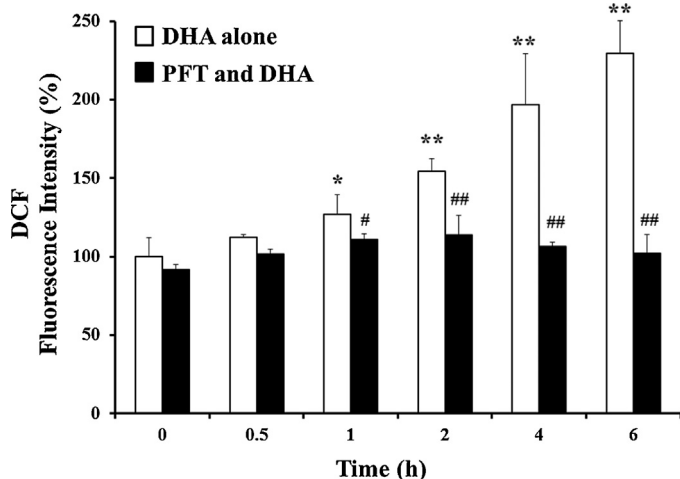

Fig. 2. Effects of PFT on DHA-induced cytotoxicity in Hep3B (p53 null) or Huh7 (p53 mutant) cells. Cells were pre-treated for 1 h with 20 μM PFT, followed by addition of DHA at the indicated concentrations to culture medium, and further incubation for 24 h. Survival (%) was calculated relative to controls. Results are means ± SEM of three samples. White bars (□): single incubation with DHA; black bars (■): pretreatment with PFT, and incubation with DHA. $^{**}p < 0.01$ compared with controls, $^{##}p < 0.01$ compared with indicated concentrations of single incubation with DHA.

Similarly, single incubation with DHA showed concentration-dependent reductions in cell survival, and PFT significantly inhibited the cytotoxic effects of DHA in both cell types (Fig. 2). Thus, PFT abrogated DHA-induced cytotoxicity independently of p53 expression.
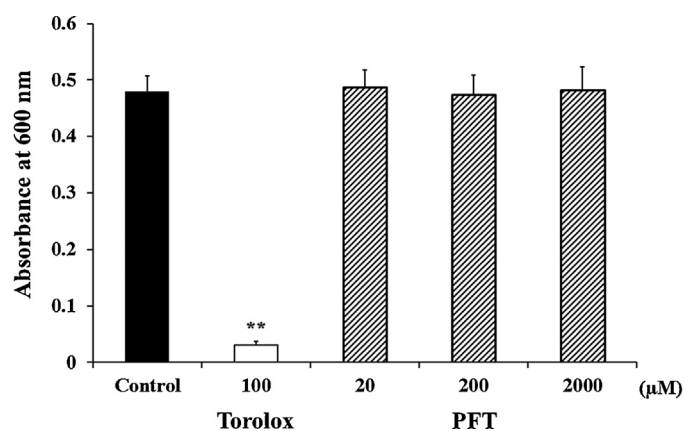
4. PFT blocked DHA-induced oxidative stress and autophagy in HepG2 cells

We examined the effects of PFT on DHA-induced oxidative stress, as indicated by DCF fluorescence (Fig. 3). Induction of oxidative stress by DHA at 120 μM was significantly elevated after 1 h of incubation ($126.8 \pm 12.8\%$; $p < 0.05$), and increased further at 2, 4 and 6 h ($154.2 \pm 8.1\%$, $196.6 \pm 32.8\%$ and $229.8 \pm 20.3\%$, respectively), as compared to controls ($p < 0.01$). These DHA-induced increase in oxidative stress were abrogated by pretreatment with PFT after incubation for 1 h ($110.8 \pm 3.6\%$; $p < 0.05$), and were further blocked by longer incubation for 2, 4 and 6 h ($113.8 \pm 12.4\%$, $106.5 \pm 2.3\%$ and $103.9 \pm 12.2\%$, respectively; $p < 0.01$). To confirm the inhibitory effects of PFT on DHA-induced oxidative stress and whether PFT has antioxidant capacity, we performed TAC assay. As shown in Fig. 4, PFT does not show antioxidant capacity when compared with Trolox, even at 2000 μM.

In order to explore the inhibition mechanisms of PFT on DHA-induced cytotoxicity, we focused on the induction of autophagy (Fig. 5). Levels of LC3A-II, which is an LC3-phosphatidyl-ethanol-amine conjugate and a promising autophagosomal marker (Asanuma et al., 2003), showed concentration-dependent increases in incubation with DHA on Western blotting (Fig. 5A and B). Expression was completely blocked by PFT. This inhibitory effect of PFT was also observed in both Hep3B and Huh7 by incubation with high concentrations of DHA at 200 μM (Fig. 5C and D). On immunofluorescence, PFT incubation for 24 h showed no changes when compared with control groups, but the DHA-treated group showed increased numbers of LC3-positive cells, and this effect was apparently blocked by pretreatment with PFT (Fig. 5E). Similarly, after transfection with pAcGFP-LC3 in HepG2 cells, PFT

Fig. 4. Total antioxidant capacity of PFT or Trolox. An oxidation system comprising 2, 2′-azino-di (3-ethylbenzthiazoline-6-sulfonic acid) (ABTS), myoglobin and hydrogen peroxide (H_2O_2) was used for TAC assay to determine Trolox equivalent antioxidant capacity, as described in Section 2. Increases in absorbance at 600 nm for 10 min were then recorded. Results are expressed as means $\pm$ SEM of three samples. Black bar (■): no incubation with reagent as control; white bar (□): incubation with Trolox at 100 μM; striped bars (▨): incubation with PFT at 20, 200 or 2000 μM. $**p < 0.01$ compared with control group.

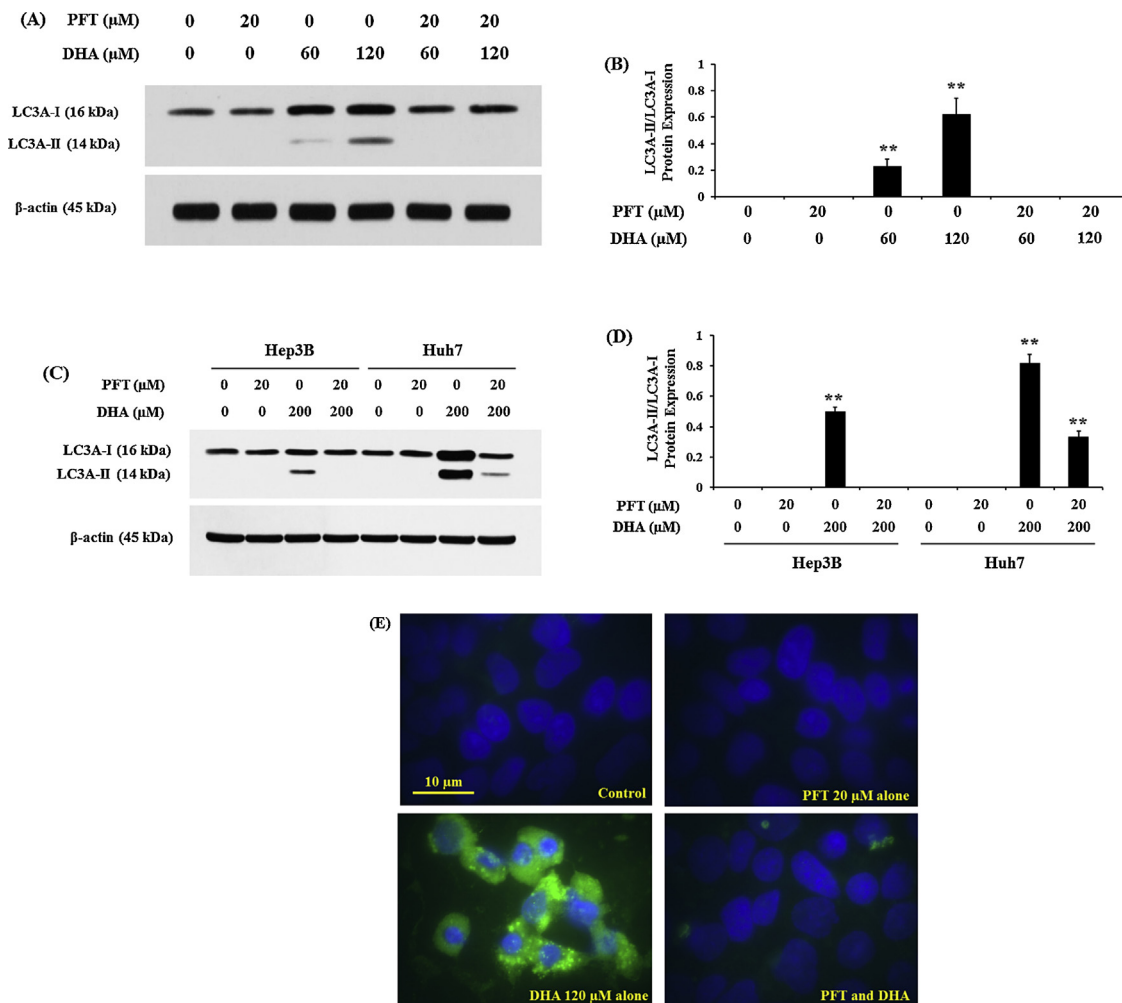blocked the formation of LC3 puncta in cells on incubation with DHA (see Supplementary data 1).

Supplementry material related to this article found, in the online version, at http://dx.doi.org/10.1016/j.toxlet.2014.11.016.

4.1. PFT decreased release of cytochrome c by DHA in HepG2 cells

Next, we examined the release of cytochrome c from mitochondria to cytosol by DHA (Fig. 6). Cytochrome c is a critical mediator of mitochondrial cell death. COX IV, a specific mitochondrial marker, was detected in mitochondrial fractions, indicating good-quality mitochondrial preparations (Fig. 6A). Cytochrome c decreased in the mitochondrial fraction and increased in the cytosol fraction after incubation with DHA. On densitometric measurement of bands on Western blotting (ratio is expressed as cytosol/mitochondria fraction), single incubation with DHA for 1 or 4 h gave ratios of 0.95 ± 0.15 or 1.33 ± 0.29 when compared with controls, and this release of cytochrome c was significantly suppressed by pretreatment with PFT (0.56 ± 0.04, $p < 0.01$, and 0.83 ± 0.14, $p < 0.05$, respectively; Fig. 6B). Similarly, on immunofluorescence observations, although PFT showed no changes in cytochrome c expression when compared with control groups, marked increases in cellular expression were seen after incubation with DHA and these were attenuated by pretreatment with PFT (Fig. 6C). Thus, PFT showed significant suppression of cytochrome c release from mitochondria to cytosol.

4.2. Effects of PFT on DHA-induced changes in mitochondrial membrane potential ($\Delta \Psi_M$).

In order to further investigate the mechanisms of cell death in our study, we examined whether there were any changes in $\Delta \Psi_M$ resulting in the stimulation of mitochondrial cell death. We analyzed the effects on $\Delta \Psi_M$ using the JC-10 dyes (Fig. 7). JC-10 is a membrane-permeable fluorescent dye used for the measurement of $\Delta \Psi_M$. In intact cells, JC-10 concentrates in the mitochondrial matrix where it forms orange fluorescent aggregates. However, in damaged cells, JC-10 diffuses out of mitochondria, changes to a monomeric form and stains cells to show green fluorescence. As shown in Fig. 7A, PFT increased aggregate (orange) forms, but not monomer (green) forms. The fluorescence intensity of aggregate forms was markedly higher after incubation for 1 h and persisted

Fig. 3. Effects of DHA-induced oxidative stress in HepG2 cells. Oxidative stress was estimated by 2′,7′-dichlorofluorescein (DCF) fluorescence assay, as described in Section 2. Quantitative analysis of oxidative stress by HepG2 cells incubated in the presence of DHA at 120 μM for the indicated times. Pre-treatment with PFT at 20 μM was performed for 1 h before incubation with DHA. The results are expressed as a percentage of DCF fluorescence intensity with respect to controls. Data are means $\pm$ SEM of three samples. White bars (□): single incubation with DHA; black bars (■): pretreatment with PFT and incubation with DHA. $*p < 0.05$, $**p < 0.01$ compared with controls, $\#p < 0.05$, $\#\#p < 0.01$ compared with indicated concentrations of single incubation with DHA.

Fig. 5. Effects of PFT on DHA-induced autophagy indicating LC3 expression. (A and C) Western blots analysis of LC3 expression in whole cells. Each sample ($n=3–5$) was incubated for 12 h with DHA pre-treated with or without PFT. Samples containing 30 μg of protein were loaded onto 15% SDS-PAGE gels and blots were probed with antibody. β-actin levels were used as a loading control. (B and D) Protein bands were quantified by densitometry and are expressed relative to expression levels of LC3A-II/LC3A-I. $**p < 0.01$ compared with controls. (E) Immunofluorescence observation of LC3 expression. Magnification: ×1000. Fluorescence images were taken with a Nikon microscope. Treatment with DHA at 120 μM for 12 h induced the appearance of LC3 expression (green fluorescence) and this was blocked by pretreatment with PFT. (For interpretation of the references to color in this figure legend, the reader is referred to the web version of this article.)

with incubation for up to 24 h, but there were no changes in monomer forms (see Supplementary data 2). In contrast to PFT-treated groups, DHA increased monomer forms, indicating mitochondrial dysfunction, as compared with control groups. Pretreatment with PFT partially blocked the increase in monomer forms after incubation with DHA. On quantitative analysis of the ratio of aggregate/monomer (Fig. 7B), single incubation with DHA showed concentration- and time-dependent decreases in this ratio, which indicates that DHA caused changes in $\Delta\Psi_M$ and mitochondrial damage. Single treatment with PFT significantly increased the ratio to more than two-fold the levels seen in controls ($p < 0.01$), while DHA-induced decreases in the ratio were markedly attenuated by pretreatment with PFT after each incubation period. Thus, PFT blocked DHA-induced changes in $\Delta\Psi_M$.
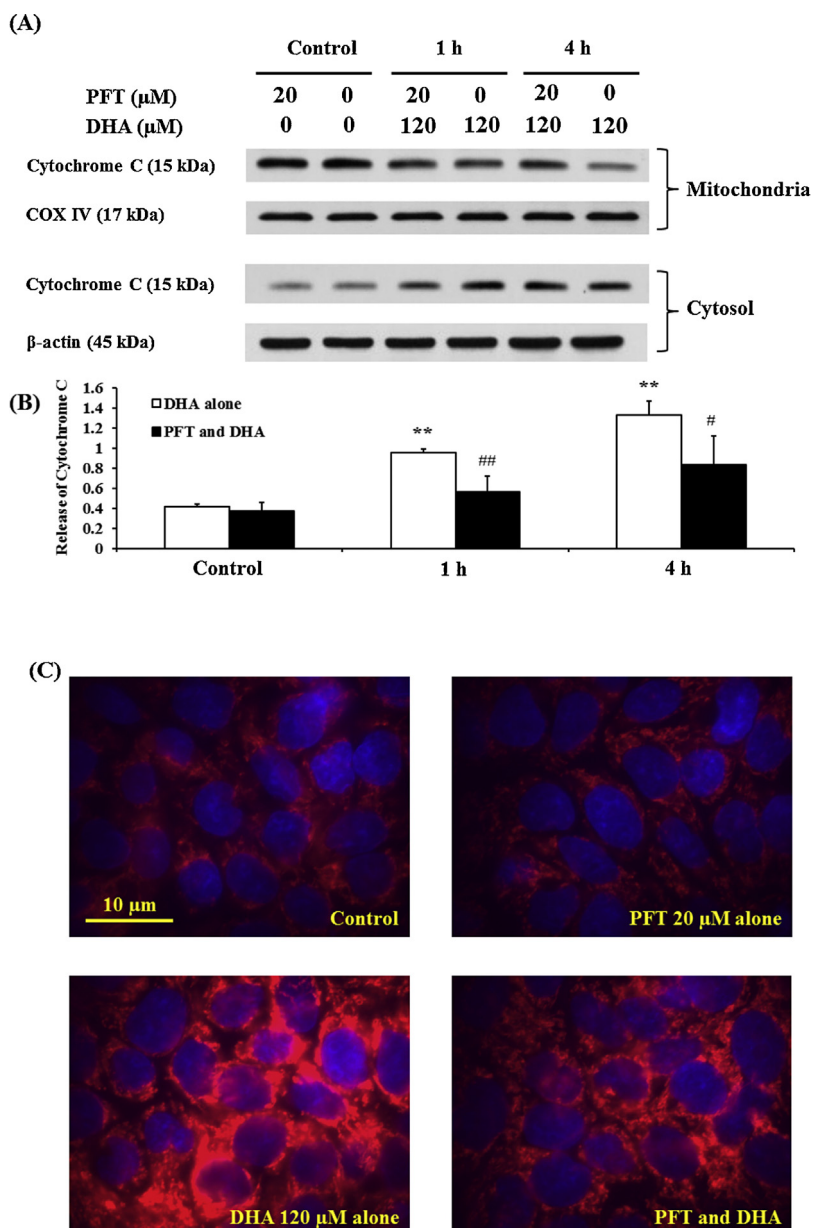
Supplementry material related to this article found, in the online version, at http://dx.doi.org/10.1016/j.toxlet.2014.11.016.

5. Discussion

Early reports identified the production of reactive oxygen species (ROS) as one of the mechanisms of DHA-induced cytotoxicity (Arita et al., 2001; Maziere et al., 1999). The

transcriptional factor p53 plays a pivotal role in cell survival and induction of ROS. In our initial hypothesis, we assumed that DHA-induced cytotoxicity was mediated through p53 activation and the subsequent signal transductions. This was based on the notion that production of ROS and disruption of mitochondria, induced by several cytotoxic agents, is associated with p53 activation (Raha and Robinson, 2000). Our previous report showed that DHA-induced cytotoxicity was mediated by induction of ROS, and antioxidants inhibited the reduction of cell survival by DHA, but this cytotoxic mechanism was not based on changes in p53 mRNA expression, total levels or phosphorylation of p53 proteins in HepG2 cells following incubation with DHA (Kanno et al., 2011). In this report, single incubation with DHA showed concentration-dependent cell survival reduction regardless of whether p53 was expressed, and PFT, a p53 inhibitor, significantly blocked DHA-induced cytotoxicity (Figs. 1 and 2). Moreover, PFT significantly blocked DHA-induced oxidative stress (Fig. 3), but it showed no antioxidant capacity on TAC assay (Fig. 4). This suggests that PFT has another, p53-independent mechanism that is not related to antioxidant capacity or ROS scavenging actions against DHA-induced cytotoxicity in HepG2 cells.

Recent evidence supports the notion that induction of autophagy occurs during the oxidative stress response (Kiffin

(A)

	Control		1 h		4 h	
PFT (μM)	20	0	20	0	20	0
DHA (μM)	0	0	120	120	120	120

Cytochrome C (15 kDa) — Mitochondria
COX IV (17 kDa)

Cytochrome C (15 kDa) — Cytosol
β-actin (45 kDa)

(B)

(C)

Fig. 6. Effects of PFT on DHA-induced release of cytochrome *c* in HepG2 cells. (A) Western blot analysis of cytochrome *c* expression in mitochondrial and cytosolic protein extracts. Cells were treated for the indicated times with DHA, with or without PFT pretreatment. Samples containing 5 μg of protein were loaded onto 15% SDS-PAGE gels and blots were probed with corresponding antibodies. β-actin levels were used to confirm the equal loading of cytosolic proteins and COX IV was used to confirm the equal loading of mitochondrial proteins. (B) Protein bands were quantified by densitometry, and are expressed relative to the expression levels of release from mitochondria to cytosol fractions. White bars (□): single incubation with DHA; black bars (■): pretreatment with PFT and incubation with DHA. $*p < 0.05$, $**p < 0.01$ compared with controls. $\#p < 0.05$, $\#\#p < 0.01$ compared with each indicated concentration of single incubation with DHA treatment group. (C) Immunofluorescence observation of cytochrome *c*. Magnification: ×1000. Fluorescence images were obtained with a Nikon microscope. Treatment with DHA at 120 μM for 4 h enhanced cytochrome *c* expression (red fluorescence), and this was attenuated by pretreatment with PFT. (For interpretation of the references to color in this figure legend, the reader is referred to the web version of this article.)

et al., 2006). In this report, DHA induced autophagy, as indicated by LC3 expression on immunofluorescence observation and Western blotting (Fig. 5). This suggests that DHA-induced autophagy is related to oxidative stress response, such as induction of ROS. Nuclear p53 positively regulates autophagy in stressed cells through transactivation of autophagy-related target genes (Liang, 2010). Jing et al. (2011) showed that inhibition of p53 increases DHA-induced autophagy and prevention of p53 degradation significantly leads to attenuation of DHA-induced autophagy, thus suggesting that DHA-induced autophagy is mediated by p53. Recently, it was shown that inhibition of p53 by PFT led to impaired activation of autophagy and enhanced chemosensitivity in HCC

during nutrient deprivation (Guo et al., 2014). In contrast, as shown in Figs. 1 and 2, PFT blocked DHA-induced cytotoxicity regardless of p53 expression. This suggests that the effects of PFT may change depending on other factors, such as experimental cell culture conditions at individual facilities.

Autophagy is relevant to energy homeostasis (Singh, 2010), and autophagy may exert its tumor-suppressing function at the subcellular level by removing defective cytoplasmic components such as damaged mitochondria (Hofer and Wenz, 2014). Mijaljica et al. (2007) suggested that autophagy occurring subsequent to cytochrome *c* release is trigged by changes in $\Delta\Psi_M$; therefore, we assumed that it plays a key role in mitochondrial damage by DHA,
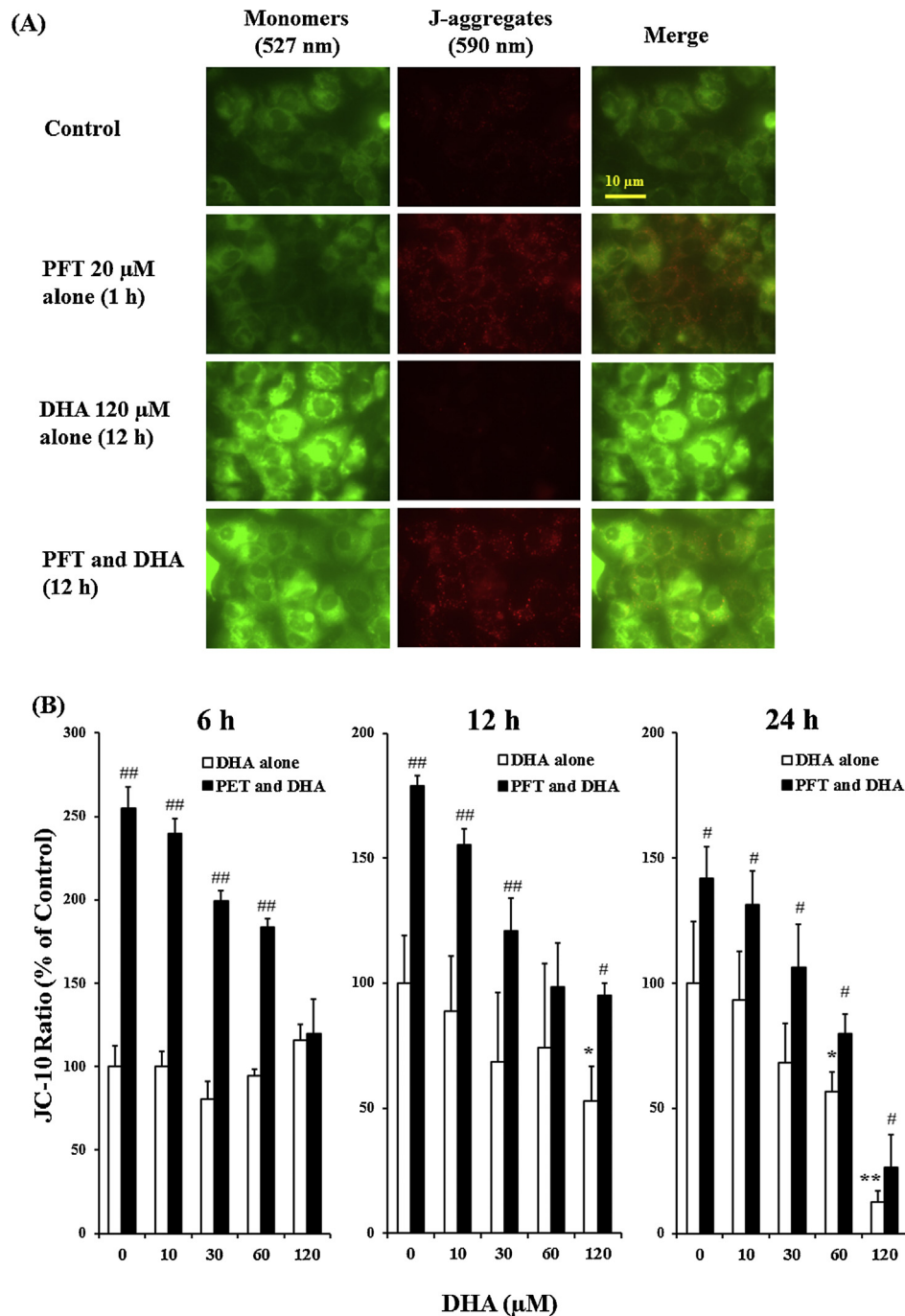
Fig. 7. Effects of PFT on DHA-induced changes in mitochondrial membrane potential ($\Delta\Psi_M$), as indicated by mitochondrial fluorescence probe JC-10. (A) Immunofluorescence observations of JC-10. Magnification: ×1000. Fluorescence images were obtained with a Nikon microscope. Pretreatment with PFT for 1 h increased J-aggregates (orange fluorescence, 590 nm) and no changes monomeric form (green fluorescence, 527 nm) were seen, as compared to control. Treatment with DHA at 120 μM for 12 h induced increases in JC-10 monomeric form, and this was attenuated by pretreatment with PFT. (B) Quantitative results of aggregate/monomer ratio were assumed to be proportional to $\Delta\Psi_M$ intensity. Results are expressed as means ± SEM of three samples. White bars (□): single incubation with DHA; black bars (■): pretreatment with PFT and incubation with DHA. $*p < 0.05$, $**p < 0.01$ compared with controls. $\#p < 0.05$, $\#\#p < 0.01$ compared with indicated concentrations of single incubation with DHA. (For interpretation of the references to color in this figure legend, the reader is referred to the web version of this article.)

and that PFT exerts some influence over mitochondria. Oxidative damage has been shown to increase the permeability of the mitochondrial membrane to various molecules and to result in mitochondrial functional failure (Kiffin et al., 2006). Changes in mitochondrial permeability are accompanied by depolarization of the mitochondrial membrane and uncoupling of oxidation and phosphorylation reactions in the mitochondrial lumen. Leakage of

intramitochondrial components, such as cytochrome *c*, constitutes the first step in activation of various cellular death programs (Assuncao Guimaraes and Linden, 2004). It should be specified that the release of cytochrome *c* (among other mitochondrial constituents) is not sufficient to trigger a cascade of apoptotic events (Luzikov, 1999). As shown in Fig. 6, PFT apparently suppressed the release of cytochrome *c* by DHA in HepG2 cells.

Thus, our results indicate that the inhibition mechanisms of PFT on DHA-induced cytotoxicity and autophagy depend on mitochondrial damage.

It has not yet been shown that mitochondria are selected for autophagy depending on the level of oxidative damage to their membranes, but some evidence suggests that mitochondrial permeability plays a role in the initiation of autophagy (Lemasters et al., 2002; Mijaljica et al., 2007). As shown in Fig. 7, single incubation with DHA showed concentration- and time-dependent decreases in $\Delta\Psi_M$ after incubation for 12 h. Fig. 3 and our previous report (Kanno et al., 2011) show that DHA-induced oxidative stress significantly increases after incubation, and release of cytochrome c increases after incubation with DHA (Fig. 6). Interestingly, changes in $\Delta\Psi_M$ by DHA were not observed before the detection of oxidative stress and release of cytochrome c; changes in $\Delta\Psi_M$ occur in a comparatively later stage of DHA treatment. JC-1 (prototype of JC-10) is reported to be a more reliable indicator of $\Delta\Psi_M$ than other dyes (Mathur et al., 2000), and it has been indicated that J-aggregate-forming lipophilic cations might be useful for probing $\Delta\Psi_M$ in living cells (Reers et al., 1995). In this study, pretreatment with PFT increased in J-aggregate formation under basal cellular conditions (Fig. 7). It has been demonstrated that $\Delta\Psi_M$ controls ROS production (Sanderson et al., 2013). Several reports have shown that chemical reagent-induced elevation of $\Delta\Psi_M$ reduces ROS production and indicates a cytoprotective effect. $(-)$ Deprenyl is an irreversible inhibitor of monoamine oxidase-B, which protects cells from hypoxia/re-oxygenization, maintains $\Delta\Psi_M$ and prevents increases in ROS induced by hypoxia/re-oxygenation in a dose-dependent manner (Simon et al., 2005). 1,2-Dimethylhydrazine treatment increases the formation of J-aggregate at higher $\Delta\Psi_M$, decreases ROS function and restricts cell death (Saini and Sanyal, 2012). These reports suggest that higher $\Delta\Psi_M$ protects ROS production and results in the prevention of ROS-mediated cytotoxicity. We speculate that PFT activates $\Delta\Psi_M$ in living cells, thereby increasing the threshold of sensitivity produced by DHA-induced oxidative stress. Thus, PFT may protect against mitochondrial damage by DHA. It is conceivable that increases in J-aggregate represent respiration or energy synthesis hot spots in the cells and may protect against cellular injury by DHA. It is unclear how PFT affects mitochondria and increases J-aggregate, and we are therefore studying this issue further.

6. Conclusion

Based on the present results, we propose the following mechanism for the effects of PFT against DHA-induced cytotoxicity. First, pretreatment with PFT protects against DHA-induced mitochondria damage by increasing $\Delta\Psi_M$ in living cells. Second, PFT blocks the increase in oxidative stress and the release of cytochrome c from mitochondria into the cytosol by DHA, but it does not show antioxidant action under the present experimental conditions. Hence, PFT inhibits mitochondrial damage and induction of autophagy-mediated oxidative stress by DHA, resulting in abrogation of DHA-induced cytotoxicity. However, it is uncertain whether the pharmacological mechanisms of PFT on mitochondrial function are fully p53 independent. Further studies are necessary in order to clarify the molecular mechanisms of PFT on DHA-induced cytotoxicity.

Conflicts of interest

The authors declare that they have no conflicts of interest.

Transparency document

The Transparency document associated with this article can be found in the online version.

References

Arita, K., Kobuchi, H., Utsumi, T., Takehara, Y., Akiyama, J., Horton, A.A., Utsumi, K., 2001. Mechanism of apoptosis in HL-60 cells induced by n-3 and n-6 polyunsaturated fatty acids. Biochem. Pharmacol. 62, 821–828.

Asanuma, K., Tanida, I., Shirato, I., Ueno, T., Takahara, H., Nishitani, T., Kominami, E., Tomino, Y., 2003. MAP-LC3, a promising autophagosomal marker, is processed during the differentiation and recovery of podocytes from PAN nephrosis. FASEB J. 17, 1165–1167.

Assuncao Guimaraes, C., Linden, R., 2004. Programmed cell deaths: apoptosis and alternative deathstyles. Eur. J. Biochem. 271, 1638–1650.

Berridge, M.V., Herst, P.M., Tan, A.S., 2005. Tetrazolium dyes as tools in cell biology: new insights into their cellular reduction. Biotechnol. Annu. Rev. 11, 127–152.

Dong, X.X., Wang, Y.R., Qin, S., Liang, Z.Q., Liu, B.H., Qin, Z.H., Wang, Y., 2012. p53 mediates autophagy activation and mitochondria dysfunction in kainic acid-induced excitotoxicity in primary striatal neurons. Neuroscience 207, 52–64.

Droge, W., 2002. Free radicals in the physiological control of cell function. Physiol. Rev. 82, 47–95.

Gleissman, H., Yang, R., Martinod, K., Lindskog, M., Serhan, C.N., Johnsen, J.I., Kogner, P., 2010. Docosahexaenoic acid metabolome in neural tumors: identification of cytotoxic intermediates. FASEB J. 24, 906–915.

Guo, J.Y., Xia, B., White, E., 2013. Autophagy-mediated tumor promotion. Cell 155, 1216–1219.

Guo, X.L., Hu, F., Zhang, S.S., Zhao, Q.D., Zong, C., Ye, F., Guo, S.W., Zhang, J.W., Li, R., Wu, M.C., Wei, L.X., 2014. Inhibition of p53 increases chemosensitivity to 5-FU in nutrient-deprived hepatocarcinoma cells by suppressing autophagy. Cancer Lett. 346, 278–284.

Hajjaji, N., Bougnoux, P., 2013. Selective sensitization of tumors to chemotherapy by marine-derived lipids: a review. Cancer Treat. Rev. 39, 473–488.

Hofer, A., Wenz, T., 2014. Post-translational modification of mitochondria as a novel mode of regulation. Exp. Gerontol. 56, 202–220.

Jing, K., Song, K.S., Shin, S., Kim, N., Jeong, S., Oh, H.R., Park, J.H., Seo, K.S., Heo, J.Y., Han, J., Park, J.I., Han, C., Wu, T., Kweon, G.R., Park, S.K., Yoon, W.H., Hwang, B.D., Lim, K., 2011. Docosahexaenoic acid induces autophagy through p53/AMPK/mTOR signaling and promotes apoptosis in human cancer cells harboring wild-type p53. Autophagy 7, 1348–1358.

Kambayashi, Y., Binh, N.T., HWA, Hibino, Y., Hitomi, Y., Nakamura, H., Ogino, K., 2009. Efficient assay for total antioxidant capacity in human plasma using a 96-well microplate. J. Clin. Biochem. Nutr. 44, 46–51.

Kanno, S., Kurauchi, K., Tomizawa, A., Yomogida, S., Ishikawa, M., 2011. Albumin modulates docosahexaenoic acid-induced cytotoxicity in human hepatocellular carcinoma cell lines. Toxicol. Lett. 200, 154–161.

Kiffin, R., Bandyopadhyay, U., Cuervo, A.M., 2006. Oxidative stress and autophagy. Antioxid. Redox Signal. 8, 152–162.

Komarova, E.A., Gudkov, A.V., 1998. Could p53 be a target for therapeutic suppression? Semin. Cancer Biol. 8, 389–400.

Komarova, E.A., Neznanov, N., Komarov, P.G., Chernov, M.V., Wang, K., Gudkov, A.V., 2003. p53 inhibitor pifithrin alpha can suppress heat shock and glucocorticoid signaling pathways. J. Biol. Chem. 278, 15465–15468.

Lemasters, J.J., Qian, T., He, L., Kim, J.S., Elmore, S.P., Cascio, W.E., Brenner, D.A., 2002. Role of mitochondrial inner membrane permeabilization in necrotic cell death, apoptosis, and autophagy. Antioxid. Redox Signal. 4, 769–781.

Liang, C., 2010. Negative regulation of autophagy. Cell Death Differ. 17, 1807–1815.

Lim, K., Han, C., Dai, Y., Shen, M., Wu, T., 2009. Omega-3 polyunsaturated fatty acids inhibit hepatocellular carcinoma cell growth through blocking beta-catenin and cyclooxygenase-2. Mol. Cancer Ther. 8, 3046–3055.

Luzikov, V.N., 1999. Quality control: from molecules to organelles. FEBS Lett. 448, 201–205.

Mathur, A., Hong, Y., Kemp, B.K., Barrientos, A.A., Erusalimsky, J.D., 2000. Evaluation of fluorescent dyes for the detection of mitochondrial membrane potential changes in cultured cardiomyocytes. Cardiovasc. Res. 46, 126–138.

Maziere, C., Conte, M.A., Degonville, J., Ali, D., Maziere, J.C., 1999. Cellular enrichment with polyunsaturated fatty acids induces an oxidative stress and activates the transcription factors AP1 and NFkappaB. Biochem. Biophys. Res. Commun. 265, 116–122.

Mijaljica, D., Prescott, M., Devenish, R.J., 2007. Different fates of mitochondria: alternative ways for degradation? Autophagy 3, 4–9.

Raha, S., Robinson, B.H., 2000. Mitochondria, oxygen free radicals, disease and ageing. Trends Biochem. Sci. 25, 502–508.

Raza, A., Sood, G.K., 2014. Hepatocellular carcinoma review: current treatment, and evidence-based medicine. World J. Gastroenterol. 20, 4115–4127.

Reers, M., Smiley, S.T., Mottola-Hartshorn, C., Chen, A., Lin, M., Chen, L.B., 1995. Mitochondrial membrane potential monitored by JC-1 dye. Methods Enzymol. 260, 406–417.

Rovito, D., Giordano, C., Vizza, D., Plastina, P., Barone, I., Casaburi, I., Lanzino, M., De Amicis, F., Sisci, D., Mauro, L., Aquila, S., Catalano, S., Bonofiglio, D., Ando, S., 2013. Omega-3 PUFA ethanolamides DHEA and EPEA induce autophagy through PPARgamma activation in MCF-7 breast cancer cells. J. Cell Physiol. 228, 1314–1322.

Rubio, N., Coupienne, I., Di Valentin, E., Heirman, I., Grooten, J., Piette, J., Agostinis, P., 2012. Spatiotemporal autophagic degradation of oxidatively damaged organelles after photodynamic stress is amplified by mitochondrial reactive oxygen species. Autophagy 8, 1312–1324.

Saini, M.K., Sanyal, S.N., 2012. PTEN regulates apoptotic cell death through PI3-K/Akt/GSK3beta signaling pathway in DMH induced early colon carcinogenesis in rat. Exp. Mol. Pathol. 93, 135–146.

Sanderson, T.H., Reynolds, C.A., Kumar, R., Przyklenk, K., Huttemann, M., 2013. Molecular mechanisms of ischemia-reperfusion injury in brain: pivotal role of the mitochondrial membrane potential in reactive oxygen species generation. Mol. Neurobiol. 47, 9–23.

Simon, L., Szilagyi, G., Bori, Z., Telek, G., Magyar, K., Nagy, Z., 2005. Low dose $(-)$ deprenyl is cytoprotective: it maintains mitochondrial membrane potential and eliminates oxygen radicals. Life Sci. 78, 225–231.

Singh, R., 2010. Autophagy and regulation of lipid metabolism. Results Probl. Cell Differ. 52, 35–46.

Wendel, M., Heller, A.R., 2009. Anticancer actions of omega-3 fatty acids–current state and future perspectives. Anticancer Agents Med. Chem. 9, 457–470.

Yao, Q.H., Zhang, X.C., Fu, T., Gu, J.Z., Wang, L., Wang, Y., Lai, Y.B., Wang, Y.Q., Guo, Y., 2014. Omega-3 polyunsaturated fatty acids inhibit the proliferation of the lung adenocarcinoma cell line A549 in vitro. Mol. Med. Rep. 9, 401–406.

Yu, T.W., Ong, C.N., 1999. Lag-time measurement of antioxidant capacity using myoglobin and 2,2′-azino-bis(3-ethylbenzthiazoline-6-sulfonic acid): rationale, application, and limitation. Anal. Biochem. 275, 217–223.

Zhu, B.S., Xing, C.G., Lin, F., Fan, X.Q., Zhao, K., Qin, Z.H., 2011. Blocking NF-kappaB nuclear translocation leads to p53-related autophagy activation and cell apoptosis. World J. Gastroenterol. 17, 478–487.